FOREX Publication
Open Access | Rapid and quality publishing

International Journal of
Electrical and Electronics Research (IJEER)
Research Article | Volume 12, Issue 3 | Pages 889-895 | e-ISSN: 2347-470X

Field Analysis and Equivalent Circuit Parameters of Linear Induction Motor with Eddy Current Secondary, Taking End Effect into Consideration

Ramadan Abdellah Ahmed[1*], M. A. Elwany[2], and A. B. Kotb[3]

[1] *Department of Electrical Engineering, Faculty of engineering, Alazhar university, Cairo, Egypt; ramadan.refaey99@gmail.com*
[2]*Department of Electrical Engineering, Faculty of Engineering, Al-Azhar University, Cairo, Egypt; MahmoudHosain1712.el@azhar.edu.eg*
[3]*Department of Electrical Engineering, Faculty of Engineering, Al-Azhar University, Cairo, Egypt; moabdelsamie45@yahoo.com*

*__Correspondence:__ Ramadan Abdellah Ahmed; *ramadan.refaey99@gmail.com*

ABSTRACT- The field analysis of a single-sided linear induction motor (LIM) taking end effect into consideration is carried out. A suitable model is used to establish the two components of secondary current density and the air gap field intensity, these components, beside the force density are carried out through the three regions model. The drive force acting on a conducting secondary sheet is calculated and plotted as functions of the speed, taking the length of secondary ends as parameter. The motor speed can be controlled by changing the displaced angle φ of the electric loading wave in the second stator phase. The equivalent circuit parameters are determined here in terms of the machine geometry by a new suggested method. These parameters are plotted as function of the motor speed for different secondary ends.

Keywords: secondary eddy current, air-gap, field analysis, motor performance, equivalent circuit parameters.

ARTICLE INFORMATION

Author(s): Ramadan Abdellah Ahmed, M. A. Elwany and A. B. Kotb;

Received: 24/06/2024; **Accepted**: 22/07/2024; **Published**: 10/08/2024;
e-ISSN: 2347-470X;
Paper Id: IJEER 2406-18;
Citation: 10.37391/ijeer.120320
Webpage-link:
https://ijeer.forexjournal.co.in/archive/volume-12/ijeer-120320.html

Publisher's Note: FOREX Publication stays neutral with regard to Jurisdictional claims in Published maps and institutional affiliations.

1. INTRODUCTION

An eddy current secondary of LIM is a smooth conducting sheet, covered by an iron one. The back iron sheet is used here to decrease the magnetic reluctance and the effective air gap length. Also, the homogenous secondary construction, allows higher linear speeds compared with the similar conventional slotted secondary, an important application of a LIM is in transportation [1]. The synchronous velocity of LIM is function of the pole pitch and does not depend on the number of stator poles.

Some authors are neglected longitudinal end effects [2]. Moreover, a long air gap length of LIM, weakens the longitudinal end effects [6]. In some types of applications, the out hangs of the secondary sheet are long compared with the active length, the lateral end effects will be also of minor importance [9]. A field analysis, using the effects of secondary sheet design on the LIM performance without taking secondary ends [10]. Other authors have carried out experimental studies on a drag cup machine to only determine the rotor resistance [8].

In this paper, the distributed stator winding is replaced by an equivalent continuous current sheet carrying the stator electric loading, The field analysis of an eddy current secondary LIM *figure 1*, is carried out using Maxwell's field equations. The current density through the secondary sheet is allowed to have longitudinal component J_z and lateral component J_x. The longitudinal distribution of the air gap flux density as well as the secondary current density components are plotted for different secondary ends. The performance characteristics are calculated and discussed, considering the influence of end effects.

1.1 Methodology

In this paper the following items will be made by choosing a suitable model for secondary end effects, a new model for taking the outer field in the secondary ends into consideration and obtaining the driving force with different secondary ends.

- Electromagnetic field equations analysis and equivalent circuit.
- Distribution for current density and air-gap flux density at different speeds with and without ends.
- Distribution of the force density with the secondary sheet length at different speeds.

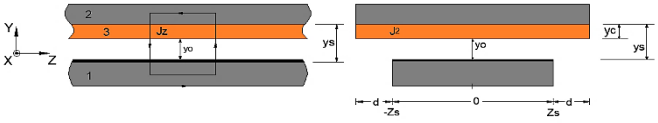

Figure 1. LIM with eddy current secondary (1-The stator, 2-Secondary iron core and, 3- Secondary sheet)

FOREX Publication
Open Access | Rapid and quality publishing
International Journal of Electrical and Electronics Research (IJEER)
Research Article | Volume 12, Issue 3 | Pages 889-895 | e-ISSN: 2347-470X

A new technique is suggested to determining the secondary equivalent circuit parameters. This applied method has taken the secondary ends and skin effect into account. The excitation system which produces the traveling magnetic field consists of two poly phase windings. The electric loading and the flux density waves are functions of time t, pole pitch τ and the lateral length x.

In this analysis, the stator electric loading of the first stator phase can be expressed in complex form as,

$$As_1 (x, t) = Re \{Am (z) ej(\omega t-ax)\} \quad (1)$$

the complex amplitude is related to that of the first stator phase

$$\text{by} \quad As_2 = As_1 e\text{-}j \varphi, \quad (2)$$

The stator electric loading is then,

$$As = As_1 + As_2 = As1 \{1 + C_{21} ej\varphi)\} \quad (3a)$$

and the ratio of the currents in the two phases is

$$C_{21} = IS_2 / IS_1. \quad (3b)$$

A pure traveling field is obtained only when the two-phase windings are supplied from a balanced two-phase source that is, when $\varphi = \pm \frac{\pi}{2}$. In this case the complex amplitude of the resultant stator electric loading reduces to

$$A_s = -j\frac{2W_S k_w}{P \tau}\sqrt{2}\, I_S, \quad (3c)$$

On the other hand, the stator electric loading turns to be pure pulsating one, when the current in one of the two phases reduces to *zero*.

2. FIELD ANALYSIS AND SUGGESTED MODEL

2.1 Analysis of Eddy Current Secondary

A model shown in *figure 1* will be used for the field analysis of (LIM) with exciting the stator side. In this model, the following assumptions are introduced to simplify the analysis:

(a) The stator winding is replaced by an equivalent current sheet of infinitesimal thickness carrying the stator electric loading A_s and placed on smooth iron surface.
(b) Both stator and secondary iron parts have infinitely permeability and zero conductivity,
(c) The air gap flux density has only y-component B_y and the secondary current has both z- and x-components.

2.2 The General Field Equations

According to the above assumptions, the air gap flux density has only y-component and the secondary current density has both z- and x-components. By applying the integral form of the Maxwell's first equation to the closed loop of infinitesimal dimensions of *figure 1*, in the *x, y-plane* yielding,

$$\frac{\partial B_y}{\partial x} = \frac{\mu_0}{y_s} A_s + \frac{\mu_0}{y_s} . y_r J_z . \quad (4a)$$

To give

$$B_y = j\frac{\mu_0}{ay_s} A_s + j\frac{\mu_0}{ay_s} . y_r J_z \quad (4b)$$

The current density in an isotropic medium moving with a velocity $\vec{v}$, is given by $\vec{J} = \sigma (\vec{E} + \vec{v} \times \vec{B})$ (5a)

where $\vec{E}$ is the electric field intensity induced by a transformer action.

The Maxwell's second equation can be applied to the shown loop in the Fig. 1b through the z, x-plane to give

$$\frac{\partial E_z}{\partial x} - \frac{\partial E_x}{\partial z} = \frac{\partial B_y}{\partial t} \quad (5b)$$

From the above equations, the magnetic flux density in the air-gap of LIM with eddy current secondary sheet is governed by the differential equation

$$\frac{\partial^2 B_y}{\partial x^2} + \frac{\partial^2 B_y}{\partial z^2} - \sigma \mu_0 \frac{y_r}{y_s} \left(\frac{\partial B_y}{\partial t} + v_x \frac{\partial B_y}{\partial x}\right) = \frac{\mu_0}{y_s}\frac{\partial A_s}{\partial x} \quad (5c)$$

The restriction to steady state operation, allows the representation of the field quantities in terms of waves like the exciting electric loading wave. Thus,

$$B_y (x,z,t) = Re \left\{\underline{B_y} (z)\, e^{j(\omega t - a x)}\right\} \quad (6a)$$

$$J_z (x,z,t) = Re \left\{\underline{J_z} (z) e^{j(\omega t - a x)}\right\} \quad (6b)$$

Substituting *Eq. (6)* into *Eq (5)* yields a second order differential equation for the complex amplitude of the air gap flux density

$$\frac{d^2 \underline{B_y}}{dz^2} - (a^2 + j\, sw\, \sigma\mu_0 \frac{y_r}{y_s})\underline{B_y} = -ja\, \frac{\mu_0}{y_s} \underline{A_s} \quad (7)$$

From (2c), a second order differential equation for the complex amplitude of the secondary current density is

$$\partial^2 J_Z / \partial z^2 - (a^2 + js\omega\, \sigma\mu_0 y_r/y_s) J_z = j\, s\, \omega\, \sigma\mu_0 A_s/y_s \quad (8a)$$

which can be given in the form,

$$\partial^2 J_Z / \partial z^2 - k^2 J_z = C \quad (8b)$$

$$\text{where, } K^2 = (a^2 + j\, s\, \omega\, \sigma\mu_0 \frac{y_r}{y_s}) \text{ and } C = j\, s\, \omega\, \sigma\mu_0\, {}_s/y_s \quad (8c)$$

The continuity condition of the current density, div $\vec{J}$ = 0.0, yields the relation between x-and z- components of secondary current density,

$$\frac{\partial J_z}{\partial z} + \frac{\partial J_x}{\partial x} = 0.0 \quad (9a)$$

Then, the complex amplitude of x-component is obtained as,

$$J_x = -j\, a\, \frac{\partial J_z}{\partial z} \quad (9b)$$

The above differential *equation (8)*, describes the longitudinal secondary current density within the stator active length ($-zs \le z \le zs$).

FOREX Publication
Open Access | Rapid and quality publishing
International Journal of Electrical and Electronics Research (IJEER)
Research Article | Volume 12, Issue 3 | Pages 889-895 | e-ISSN: 2347-470X

2.3. Solution of the Field Equations in 3-Regions Model

A model shown in *figure 2*, will be used for the field analysis of (LIM) with the secondary is extended outside the stator active length. In this model, an approximate estimation of the field outside the stator active region, ($z \leq - z_s$ and $z \geq z_s$) is introduced by assuming modified profile of the stator iron in the lateral end regions [3]. To avoid this difficulty and to simplify the analysis, an equivalent longer air gap length $y_e \geq y_s$ is introduced in the secondary end regions. Thus, the model will consist of three regions in the longitudinal direction and the air gap length of the end regions is estimated to be

$$y_e = y_s + 0.62\ d \qquad (10a)$$

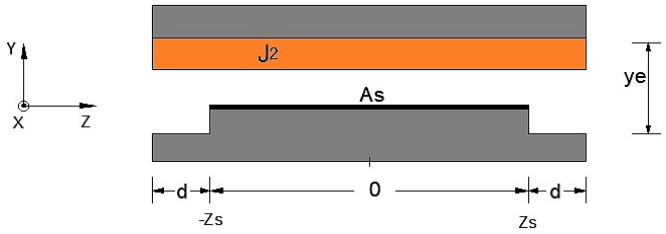

Figure 2. model of the LIM with secondary ends

The complex quantities of *equations (8c)*, must be modified to be

$$Ke_2 = (a^2 + j\ s\ \omega\ \sigma\mu_0\ yr/ye) \text{ and } Ce = 0.0 \qquad (10b)$$

2.4 General Solution

The general solution of non-homogenous second order differential *equation (8b)*, must contains the complementary function and the integral, then the solution in medium region J_{zm} is

$$J_{zm} = D_1 e^{k z} + D_2 e^{-k z} - C/K^2 \qquad (11a)$$

In determining the lateral component of the current density according to *equation (9b)*, it is more convenient to use expressions analogous to those of the longitudinal component,

$$J_{xm} = - jk/a\ (D_1 e^{kz} - D_2 e^{-kz}) \qquad (11b)$$

The air gap flux density can be determined by using (4),

$$B_{ym} = j\frac{\mu_0}{ay_s} A_s + j\frac{\mu_0}{ay_s} y_r (D_1 e^{k z} + D_2 e^{-k z} - C/K^2) \qquad (11c)$$

As there is no electric loading excitation in the secondary end regions (Ce = 0), so that the solution of Jze reduces to only the complementary function,

$$J_{ze1} = D_3 e^{ke z} + D_4 e^{-ke z} \qquad (12a)$$

$$J_{ze2} = D_5 e^{ke z} + D_6 e^{-ke z} \qquad (12b)$$

$$J_{xe1} = - jk_e/a\ (D_3 e^{ke z} - D_4 e^{-ke z}) \qquad (12c)$$

$$J_{xe2} = - jk_e/a\ (D_5 e^{ke z} - D_6 e^{-ke z}) \qquad (12d)$$

$$B_{ye1} = j\frac{\mu_0}{ay_s} . y_r J_{ze1} \qquad (12e)$$

$$B_{ye2} = j\frac{\mu_0}{ay_s} . y_r J_{ze2} \qquad (12f)$$

2.5 The Boundary Conditions

All the equations of the unknown six integration constants will be obtained from the condition of continuity of the secondary current density components (Jz, Jx).

(1) The first condition is based on that the longitudinal current density must vanish at the secondary end edges then,

at z = -(zs + d), Jze1 = 0.0 and at z = (zs + d), Jze2 = 0.0

(2) The conditions of continuity of both current density components at the ends of the active stator region yields

at z = -zs, Jze1 = Jzm, Jxe1 = Jxm (13a, b)

and at z = zs, Jze2 = Jzm, Jxe2 = Jxm (13c,d)

Substituting the solutions of the current density components in the above six equations, we obtain all the integration constants.

3. LONGITUDINAL FIELD DISTRIBUTIONS

3.1 Distribution of By, *Jz* and *Jx* with and without Secondary Ends

The computed air gap flux density and the current density components are shown in *figure 3* and *figure 4*, for the LIM with and without secondary ends. The flux density is thereby normalized by its no load value in the medium region Bo = μo A_s/ays and the current density is normalized by the theoretical quantity, Jo = As/yr. The design data are:

(2Zs = 20 cm, τ = 20 cm, yr = 5 mm, yo = 2 mm, ys = yr + yo, d = 5 cm, ye = ys + 0.62 d)

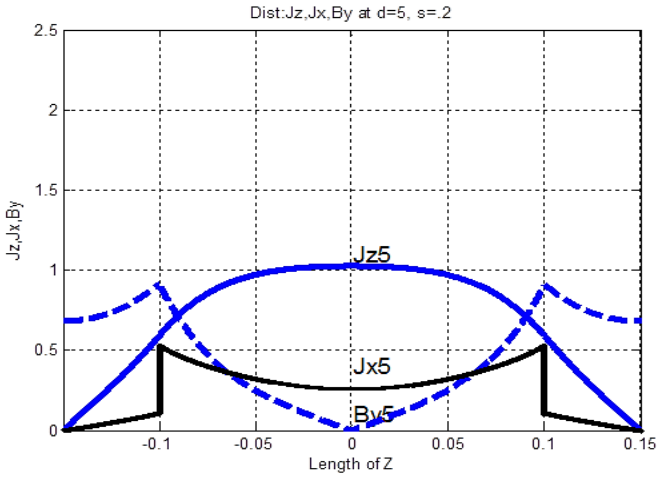

Figure 3. distribution of air gap flux density and the current density components of LIM with secondary ends

FOREX Publication
Open Access | Rapid and quality publishing
International Journal of Electrical and Electronics Research (IJEER)
Research Article | Volume 12, Issue 3 | Pages 889-895 | e-ISSN: 2347-470X

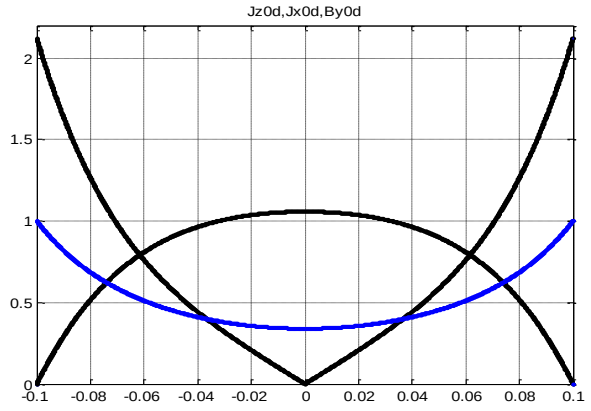

Figure 4. The distribution of the air gap flux density and the current density components of LIM without ends.

With equal secondary ends, the distributions of the air gap flux density and the two current density components are symmetrical with respect to the stator center. The point of minimum flux density and lateral current density as well as that of maximum longitudinal current density is a middle point of the stator active length, at z = 0.0As a result of the distribution of the exciting stator electric loading, the distributions of the air gap flux density and the current density components are symmetrical with respect to the stator center for equal secondary outages. The flux density as well as the lateral current density exhibit minimum values at the middle of the stator.

3.2 Force Density Distributions

The force density acting on a unit volume of the secondary can be obtained by

$$f_v = J \times B \qquad (14)$$

we are interested here for the driving force component which is obtained by

$$f_{vx} = \frac{1}{2} \mathrm{Re}\ \{ J_z\ B_y \} \qquad (15a)$$

The computed longitudinal distribution of the force density is plotted in *figure 5*, with a suitable base for normalization

$$f_o = \frac{1}{2} B_o J_o \qquad (15b)$$

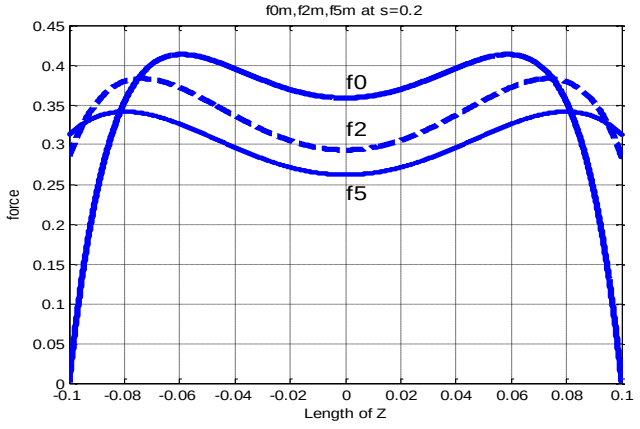

Figure 5. The longitudinal distribution of the force density, through the middle region, with different secondary ends

4. PERFORMANCE CHARACTERISTICS AND CONTROL OF LIM

4.1 Force-Slip Characteristics for Different Secondary Ends

The total developed force acting on the secondary can be obtained, by integrating the force density over the volume V of the conducting sheet,

$$F = \int_{-zs}^{zs} fv\ dv \qquad (16)$$

Figure 6, shows the force-slip characteristic for different secondary ends, with force base Fo, where

$$Fo = fo\ Vc \quad \text{and} \quad Vc = 2\ zs\ \tau\ tc. \qquad (16a,b)$$

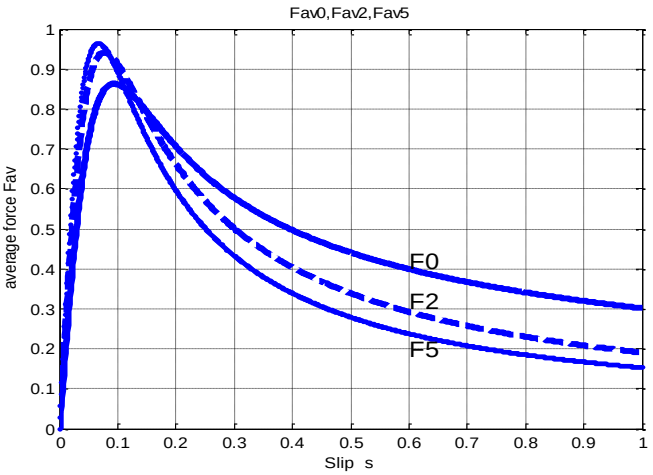

Figure 6. force-slip characteristics of LIM with different secondary ends (d = 0, 2 and 5 cm)

As shown in *figure 6*, the LIM with secondary ends has higher value for the maximum force with lower starting force. On the other hand, the LIM without secondary ends, has higher starting force but with lower value for the maximum force. Increasing the width of the overhangs improves the motor characteristics, since more current loops close their paths through the end regions. Correspondingly, longer overhangs improve the motor characteristics, as the points of maximum force density moves toward the secondary ends and increases the developed force.

4.2 Characteristics of LIM for Different Conducting Sheet Materials

As the conductivity is the measure for the machine performance characteristics, the effect of secondary sheet material conductivity is shown by *figure 7*.

The high material conductivity, improves the motor characteristics through the normal operating range, but with decreasing the starting force. This is a result of decreasing the secondary resistance which directly decreases the slip at which maximum force occurs (Sm = R2/X2).

FOREX Publication
Open Access | Rapid and quality publishing
International Journal of Electrical and Electronics Research (IJEER)
Research Article | Volume 12, Issue 3 | Pages 889-895 | e-ISSN: 2347-470X

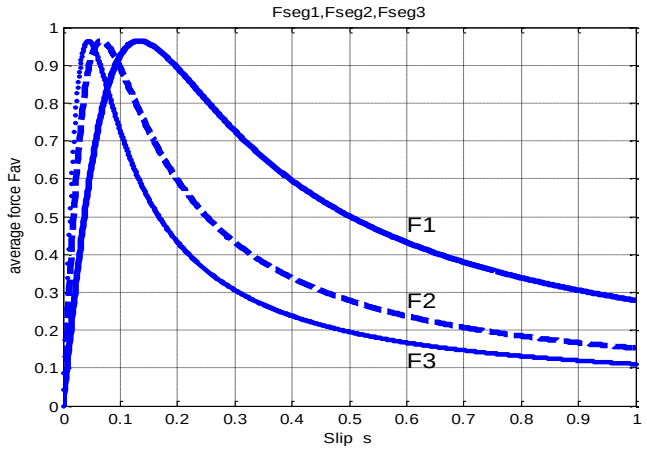

Figure 7. force-slip characteristics of LIM with different conducting Sheet Materials (σ = σn, 2 σn and 3 σn)

4.3 Phase Shifting Control for LIM

By using *equations 1, 2* of a two phase electric loadings, the force-slip characteristics are plotted in *figure 8*, for different values of the phase shift angle φ, As φ is the phase angle between the two electric loading waves of the stator phases.A pure traveling field is obtained only when the two-phase windings are supplied from a balanced two-phase source, that is, when $\varphi = \pm \frac{\pi}{2}$. A pure Pulsating field is obtained when the two-phase windings are supplied from a single-phase source that is, when φ = 0.0. On the other hand, this occurs when the stator electric loading turns to be pure pulsating one.

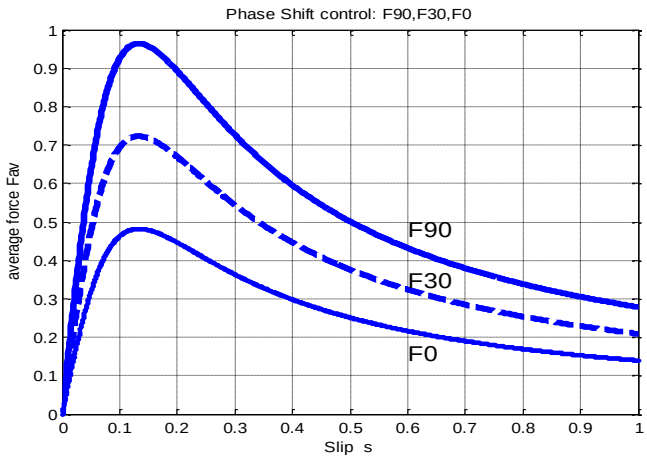

Figure 8. Force-slip characteristics with different values of phase shift angle φ (φ = 90, 60, 30 and 0.0)

It is evident that this method of speed control is associated with additional secondary losses due to the increased slip for a certain load force. The LIM speed control range remains always limited down to the speed corresponding to the maximum force.

5. DERIVATION OF THE EQUIVALENT CIRCUIT PARAMETERS

The well-known equivalent circuit of *figure 13*, is proposed to represent the induced voltage across the magnetizing reactance X_m in parallel with the secondary equivalent impedance Z_2.

The secondary impedance consists of a pure resistance (R_2/s), in series with a pure imaginary element jX_2 which represents the secondary leakage reactance.

It is obvious that, the mechanism of the secondary leakage existing in the LIM differs from that in usual slotted machine. The leakage of the eddy current conducting sheet expresses the decoupling between the secondary and the stator. It is in consequence of the fact that, some conducting sheet current elements close their paths within the active length depending on the width of the secondary ends. These ends for the eddy current secondary sheet do the job of the short circuit rings in usual squirrel cage rotors. It is then to be expected that the leakage decreases as the width of the rotor ends increase.

The equivalent secondary resistance can he obtained from the air gap power were,

$$P_g = m_s \, \mathrm{Re}\left\{ \underline{E_s} \; . \underline{I_s^*} \right\} \qquad (17a)$$

where the air gap power can be taken in the form

$$P_g = m_s \, X_m \; \beta \; . \; \underline{I_{sf}^2} \qquad (17b)$$

Also, the air gap power can be expressed in terms of the equivalent secondary current and resistance as

$$P_g = m_s \frac{R_2}{s} . \underline{I_2} . \underline{I_2^*} \qquad (17c)$$

To obtain the equivalent secondary resistance, equate the above expressions of the air gap power, with taking the equivalent secondary current I_2 in terms of the stator current I_s.

The equivalent secondary resistance can then be given

$$R_2 = \beta_r / (G.G^*) \, X_m \, s \qquad (18)$$

To obtain the equivalent secondary leakage reactance, use the voltage equation of the secondary circuit, which can be obtained in the form

$$J \, X_m \, (1 + G) + (R_2/s + j \, X_2) \, G = 0.0 \qquad (19a)$$

Separation of the real and imaginary parts results in the equivalent secondary leakage reactance

$$X2 = - (1 + Gr/(G.G^*) \, Xm \qquad (19b)$$

These two expressions enable the individual parameters of eddy current secondary equivalent circuit to be determined for any LIM design data. It provides useful guidelines for the use of designer in selecting suitable secondary dimensions to satisfy specified machine characteristics. To investigate the effects of the secondary ends on the equivalent circuit parameters, several calculations have been carried out for different machine design data. *Figures (14a) and (b)* show the equivalent secondary resistance and leakage reactance respectively.

FOREX Publication
Open Access | Rapid and quality publishing
International Journal of Electrical and Electronics Research (IJEER)
Research Article | Volume 12, Issue 3 | Pages 889-895 | e-ISSN: 2347-470X

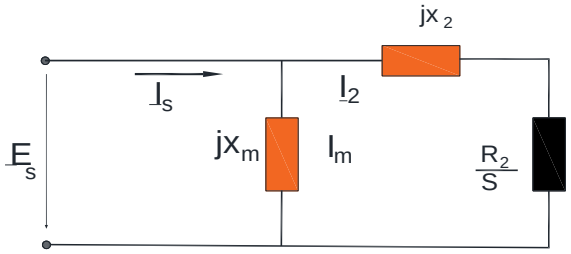

Figure 12. The proposed secondary equivalent circuit

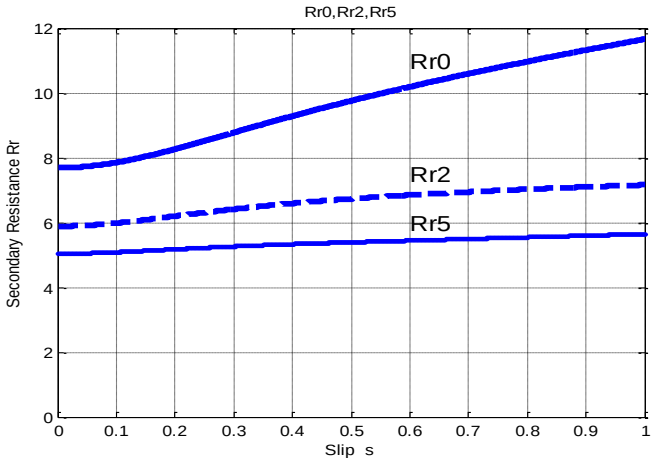

(a)

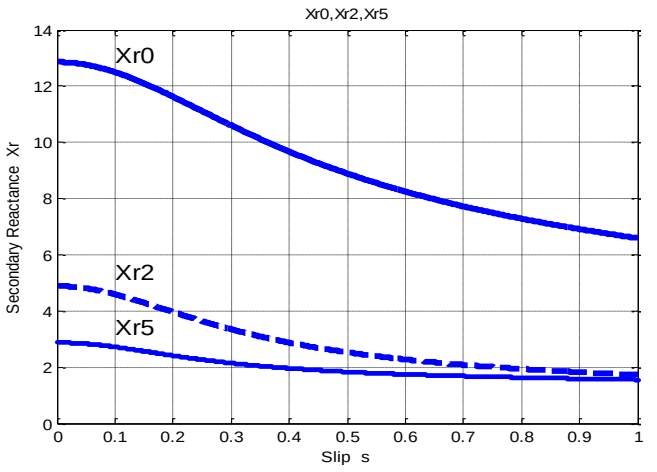

(b)

Figures 13. a and b show the equivalent secondary resistance and leak¬age reactance respectively.

The equivalent secondary resistance, is plotted in *figure (14a)* as function of the slip for three different values of the secondary end's width as parameter. The effect of the end resistances is inherently included in the expression for the equivalent secondary resistance, which increases as the end width decreases. By short ends, the secondary resistance is more affected by the speed and attains a minimum value at the synchronous speed. As the secondary ends increases, the resistance has no dependence on the machine speed and its value becomes more and more weaker. This is explained by the fact that the secondary current elements close their paths more and more through the secondary ends as the width of the ends increases. Then the important study result may be given to be, the eddy current secondary equivalent resistance, changes obviously in inverse proportion to the ends width.

The equivalent secondary reactance, is plotted in *figure (13b)* as function of the slip for three different values of the secondary end's width as parameter. the leakage reactance decreases by increasing the ends width. This behaviour is to be expected due to the nature of the eddy current secondary leakage mechanism expressing the decoupling between the secondary and the stator.

The decoupling increases as the end's width decrease; since more and more current elements close their paths within the machine active length. The leakage reactance can attain comparatively high values in the normal operating range. As function of the slip, the leakage reactance obtains a maximum value at synchronous speed, which becomes more pronounced by shorter ends.

6. CONCLUSIONS AND FUTURE WORK

The analysis of eddy current secondary linear induction motor using the field principles with special models, may need more calculation effort, but it restores the distribution of the field quantities. The two constructions for the LIM with and without ends are proposed and their models are considered considering the length of the air-gap for each case. The secondary end regions of longer overhang improve the motor characteristics, as the points of maximum force density move toward the secondary ends to increase the developed force in the normal operating range. The effect of the end resistances is inherently included in the derived expression for the equivalent secondary resistance, which increases as the end width decreases. As the secondary ends increases, the equivalent circuit parameters, has low dependence on the speed and their values become more and more weaker. This can be explained by the fact that the secondary current elements close their paths more and more through the secondary ends.

Future Work: The researcher's efforts about this point shouldn't stop until the best results for force, speed, flux and current is obtained. As future work recommendations the following points should consider:

1. Operating of two-phase LIM from single phase supply from PV system using single phase \two phase inverter.

2. Derivation equivalent circuit for two phase LIM under unbalance supply to drive the motor under traveling field.

3. Take the two components of the air gap flux to investigate the two force components (longitudinal and literal components).

REFERENCES

[1] Hughes, Austin, And Bill Drury. "Electric Motors and Drives, Fundamentals Types and Applications", Newnes 5ed 2019.

[2] Menessy, Ahmed, M. Elwany, And A. B. Kotb. "Derivation of The Circuit Parameters for A Sleeve Rotor Induction Machine." Journal of Al-Azhar University Engineering Sector 14.51 (2019): 553-558.

International Journal of
Electrical and Electronics Research (IJEER)
Research Article | Volume 12, Issue 3 | Pages 889-895 | e-ISSN: 2347-470X

[3] A. B, Kotb: "Disc-Rotor Induction Motor with Mechanical Speed-Control", Sci.Boll. Fac. Eng. Ain Shams Univ, 1996.

[4] S. E. Abdollahi, M. Mirsalim, and A. Vahedi, "Performance Analysis of a Solid Rotor Disk Induction Motor", ICEM 2004, Cracowa, Poland, sept. 2004.

[5] WEH, H., MOSEBACH, H. and MAY, H.: "Analysis and characteristics of the Disk - Rotor Induction Motor", electric machines and electro mechanics. 1, 1976, p. 87-98.

[6] HÜBNER, K.D., MOSEBACH, H. and WEH, H.: "A contribution to the calculation of the air gap field of asynchronous linear motors," Etz Archiv 93, 1972, pp. 644-646.

[7] Ahmad Shahid Khan, and Yatendra Pal Singh, "Electromagnetics for electrical machines", CRC Press, 2018.

[8] C.W. Blachford: "Induction Cup Parameters", IEEE Trans.-PAS, Vol.84, (1965) 1089-1093.

[9] Omar S. Daif, M. Helmy, "Field Analysis, Distribution and Performance of Sleeve Rotor Induction Motor Taking the Sleeve Rings into Consideration ", International Journal of Recent Technology and Engineering (IJRTE), March 2020.

[10] M. A. Elwany "Two – phase Sleeve Rotor Induction Motor Fed from Single-phase Supply", Journal of Al Azhar University Engineering sector, Vol.6, No.21, October, 2011.

[11] Salama Abo-Zaid; "Field Analysis and Equivalent Circuit Parameter of Eddy Current Rotor Induction Motor with, Without and Closed Iron Backing", IJAST, Vol. 29, No. 3, 2020,

[12] Daif, Omar & El-Raouf, M. & Esmaeel, Mohamed & Kotb, Abd. "Economic design of sleeve rotor induction motor using rotor ends. International Journal of Electrical and Computer Engineering "(IJECE), (2022).

[13] A.B. Kotb, M.Shalaby, "Analysis of the Disk Rotor Induction Motor", AMSE Confer. Vol. 2C, PP. 73-86, 1987.

[14] R. K. S. Chitroju and C. Sadarangani, "Design and analysis of asymmetrical rotor for induction motors," International Conference on Electrical Machines, Vilamoura, Portugal, 2008,

[15] Ekergård, Boel & Leijon, Mats. Longitudinal End Effects in a Linear Wave Power Generator. Energies (2020).

[16] Lu, J.-Y & Ma, W.-M & Li, L.-R." Research on longitudinal end effect of high speed long primary double-sided linear induction motor". (2008).

[17] Ahmed Samir Kheder , M. A. Elwany and A. B. Kotb3. "Analysis of Disc Motor with Asymmetrical Conducting Rotor." International Journal of Electrical and Electronics Research (IJEER)2024.